Supporting Information

Seitz and Blokesch 10.1073/pnas.1315647110

SI Materials and Methods

Bacterial Strains and Plasmids. *Vibrio cholerae* strains and complementing plasmids used throughout this study are described in Tables S2 and S3. *Escherichia coli* strain DH5α (1) was used for cloning purposes. Genomic DNA used as transforming material in the whole-cell DNA-uptake assay (2) was extracted from *E. coli* strain BL21 (DE3) (3). Bacterial mating was performed with the respective *V. cholerae* strains and *E. coli* strain S17-1λpir (4) as the donor for plasmid transfer.

Media and Growth Conditions. All bacterial strains were grown aerobically in Luria–Bertani medium (LB) at 30 °C or 37 °C. A total of 1.5% (wt/vol) agar was added to produce solid LB/agar plates. For *tfoX* expression and induction of other constructs under control of the P_{BAD} promoter the LB was supplemented with 0.02% L-arabinose (L-ara). Thiosulfate Citrate Bile Salts Sucrose (TCBS) agar plates were prepared as suggested by the manufacturer (Fluka) and used to counterselect *E. coli* after bacterial conjugation. NaCl-free LB containing 6% (wt/vol) sucrose was used for sucrose-based counterselection. If required, LB and LB/agar plates were supplemented with antibiotics at final concentrations of 50 μg/mL, 75 μg/mL, and 100 μg/mL for gentamicin, kanamycin, and ampicillin, respectively. The ampicillin concentration was lowered to 50 μg/mL for competence-induced *V. cholerae* strains.

DNA-Manipulation Techniques. Recombinant DNA techniques followed standard protocols. DNA-modifying enzymes and restriction enzymes were obtained from New England Biolabs. Taq DNA polymerase (GoTaq; Promega) and the high-fidelity Polymerase Pwo (Roche) were used for PCR amplifications. DNA sequences were verified using Sanger sequencing (Microsynth, CH).

Construction of Plasmids and Mutant Strains. All plasmids used in this study were based on pBAD/Myc-HisA (Invitrogen). This plasmid allows inducible expression from the *ara*BAD (P_{BAD}) (5) promoter upon provision of arabinose. For the amplification of *V. cholerae* DNA, the genomic DNA (gDNA) of strain A1552 (6) served as a template. Site-directed mutagenesis was performed through inverse PCR. Details of plasmid construction are listed in Table S3.

To delete genes from parental strain A1552, a gene-disruption method based either on the counter-selectable plasmid pGP-Sac28 (7) or on natural transformation and FLP recombination (TransFLP method) (8–11) was used. Strains containing fluorescent fusion constructs were first cloned into plasmids and then transferred to the chromosome, using the TransFLP method (9, 10). gDNA and plasmid DNA were consistently verified through sequencing.

V. cholerae strains carrying arabinose-inducible *tfoX* on the chromosome were constructed by triparental mating between the respective *V. cholerae* strains (Table S2) and *E. coli* strains carrying either plasmid pUX-BF13 (12) or pGP704-mTn7-*araC*-*tfoX* (13).

Primer sequences used for cloning and strain construction are available upon request.

Natural Transformation Assays. The natural transformability of bacteria grown on chitin flakes was determined as previously described (2, 8, 9). For chitin-independent transformation all strains contained an arabinose-inducible copy of *tfoX* (gene region: *araC*-P_{BAD}-*tfoX*) on the chromosome (referred to as Tn*tfoX*) (13). The transformation assays were carried out as previously published (13). gDNA of strain A1552-lacZ-Kan (8) served as the transforming material for all transformation assays. Transformation frequencies were calculated as the number of transformants divided by the total number of colony-forming units (cfu). To assess natural transformability in different growth phases, bacteria were exposed to transforming DNA solely for 30 min, which differs from the 5-h incubation time used in the standard protocol (13). Cells were subsequently treated with DNaseI (Roche) in PBS buffer containing 10 mM $MgCl_2$ for 10 min at 37 °C. Serial dilutions were plated, and the cfu were enumerated.

Detection of tDNA Uptake by Whole-Cell Duplex PCR. DNA uptake was verified using a whole-cell duplex-PCR assay as previously described (2), with slight modifications. Briefly, competence-induced bacteria were grown aerobically to an optical density at 600 nm (OD_{600}) of 1.0–1.5. Then, gDNA (2 μg/mL) of *E. coli* strain BL21 (DE3) was added, and the cells were incubated for 2 h. A DNaseI (Roche) treatment step for 15 min at 37 °C followed after the cells were harvested, and excess nuclease was removed by several wash steps. Ultimately, the bacteria were resuspended in 100 μL PBS, and ~3×10^6 bacteria served as the template in the whole-cell duplex PCR. Primer pairs were specific to the transforming DNA derived from *E. coli* strain BL21 (DE3) and the chromosome of the *V. cholerae* acceptor strain (at a 10-fold lower concentration). The latter reaction served as a control to indicate that there were equal numbers of acceptor bacteria (2).

Fluorescence Microscopy of Translational Fusion Constructs. Fluorescence microscopy was performed using a Zeiss Axio Imager M2 epifluorescence microscope. Image acquisition was performed with the Zeiss AxioVision software and a high-resolution AxioCam MRm camera. The objective used in this study was a Plan-Apochromat 100×/1.4 Oil objective. An HXP120 lamp was used for illumination. Filter sets were derived from Zeiss and included the following: 63 HE mRFP shift free and 38 Endow GFP shift free. Image processing and annotation were performed using ImageJ. All bacterial samples were mounted on 2% (wt/vol) agarose pads.

Immunofluorescence Staining and Visualization of the Competence-Induced Pilus. Pili were visualized by immunofluorescence microscopy, targeting the major pilus subunit, PilA. More precisely, *V. cholerae* strains used to study piliation carried a translational fusion between the major pilus subunit-encoding gene *pilA* and the sequence coding for the 8-aa *Strep*-tag II affinity tag (IBA) at the endogenous locus of *pilA* (*pilA*-strep). The strains were grown aerobically in LB supplemented with 0.02% L-arabinose for 6–7 h (Fig. S2). For live cell imaging, culture aliquots were incubated for 10 min with a *Strep*-tag–recognizing antibody (StrepMAB classic conjugated to Oyster 488; IBA) at a dilution of 1:250. Cells were washed once in PBS and imaged immediately.

Through a serendipitous finding, we discovered that the SNAP-Cell TMR-Star substrate (New England Biolabs) stains the membrane of *V. cholerae*, including the sheathed flagellum. Thus, for costaining of pili and flagella, bacteria were placed in a shaking incubator for 30 min with SNAP-Cell TMR-Star at a final dilution of 1 mM. Next, the bacteria were pelleted, resuspended in PBS, and fixed for 30 min with 2% (wt/vol) paraformaldehyde. After three rounds of washing, the cells were incubated for 1 h with the anti–*Strep*-tag antibody (StrepMAB Oyster 488; diluted 1:250) under

gentle agitation. The bacteria were mounted after four additional wash steps and visualized by fluorescence microscopy.

Analysis of Microscopy Images Using MicrobeTracker. The MicrobeTracker Suite (14) was used for statistical analysis of microscopy images. The parameters of Alg4 were altered slightly (splitThreshold set to 0.2 and split1 set to 1) to outline *V. cholerae* cells. The spotFinderM tool was used to quantify piliated cells. To determine the position of the pilus along the cell, the attachment point of the pilus was marked manually. The relative l-coordinates of the spots were used for statistics. Data from three biological replicates were checked for consistency and pooled for analysis.

Alignment of PilB Protein Sequences. PilB protein sequences homologous to PilB of *V. cholerae* N16961 were retrieved from the Comprehensive Microbial Resource (CMR) Web page of the J. Craig Venter Institute (http://cmr.jcvi.org/) for the following bacteria: *Myxococcus xanthus* DK 1622 (locus name: MXAN_5788), *Neisseria gonorrheae* FA1090 (Oklahoma) (locus name: NGO1673), *Haemophilus influenzae* KW20 RD (locus name: HI_0298), and *Bacillus subtilis* 168 (locus name: BSU24730). The four protein sequences were aligned using Clustal Omega (www.ebi.ac.uk/Tools/msa/clustalo). The Walker B region in Fig. S5 was highlighted according to ref. 15.

1. Yanisch-Perron C, Vieira J, Messing J (1985) Improved M13 phage cloning vectors and host strains: Nucleotide sequences of the M13mp18 and pUC19 vectors. *Gene* 33(1): 103–119.
2. Suckow G, Seitz P, Blokesch M (2011) Quorum sensing contributes to natural transformation of *Vibrio cholerae* in a species-specific manner. *J Bacteriol* 193(18): 4914–4924.
3. Studier FW, Moffatt BA (1986) Use of bacteriophage T7 RNA polymerase to direct selective high-level expression of cloned genes. *J Mol Biol* 189(1):113–130.
4. Simon R, Priefer U, Pühler A (1983) A broad host range mobilization system for *in vivo* genetic engineering: Transposon mutagenesis in Gram negative bacteria. *Nat Biotechnol* 1:784–791.
5. Schleif R (2010) AraC protein, regulation of the l-arabinose operon in *Escherichia coli*, and the light switch mechanism of AraC action. *FEMS Microbiol Rev* 34(5):779–796.
6. Yildiz FH, Schoolnik GK (1998) Role of *rpoS* in stress survival and virulence of *Vibrio cholerae*. *J Bacteriol* 180(4):773–784.
7. Meibom KL, et al. (2004) The *Vibrio cholerae* chitin utilization program. *Proc Natl Acad Sci USA* 101(8):2524–2529.
8. Marvig RL, Blokesch M (2010) Natural transformation of *Vibrio cholerae* as a tool—optimizing the procedure. *BMC Microbiol* 10:155.
9. De Souza Silva O, Blokesch M (2010) Genetic manipulation of *Vibrio cholerae* by combining natural transformation with FLP recombination. *Plasmid* 64(3):186–195.
10. Blokesch M (2012) TransFLP – a method to genetically modify *V. cholerae* based on natural transformation and FLP-recombination. *J Vis Exp* 68:e3761.
11. Borgeaud S, Blokesch M (2013) Overexpression of the *tcp* gene cluster using the T7 RNA polymerase/promoter system and natural transformation-mediated genetic engineering of *Vibrio cholerae*. *PLoS ONE* 8(1):e53952.
12. Bao Y, Lies DP, Fu H, Roberts GP (1991) An improved Tn*7*-based system for the single-copy insertion of cloned genes into chromosomes of gram-negative bacteria. *Gene* 109(1):167–168.
13. Lo Scrudato M, Blokesch M (2012) The regulatory network of natural competence and transformation of *Vibrio cholerae*. *PLoS Genet* 8(6):e1002778.
14. Sliusarenko O, Heinritz J, Emonet T, Jacobs-Wagner C (2011) High-throughput, subpixel precision analysis of bacterial morphogenesis and intracellular spatio-temporal dynamics. *Mol Microbiol* 80(3):612–627.
15. Filloux A (2004) The underlying mechanisms of type II protein secretion. *Biochim Biophys Acta* 1694(1–3):163–179.

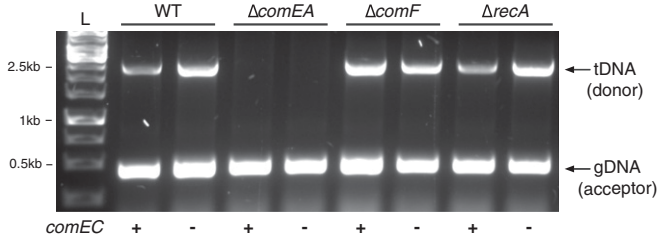

Fig. S1. Detection of internalized tDNA by whole-cell duplex PCR. DNA uptake was tested by whole-cell duplex PCR (2) in wild-type (WT) or representative mutant strains (ΔcomEA, ΔcomF, and ΔrecA) of *V. cholerae*. All strains were either wild type for *comEC* (+) or *comEC*$^{-}$ (–) as indicated below the image. The PCR reactions contained primers specific to the transforming DNA (tDNA) (2,652 bp, *Upper*) and to the genomic DNA (gDNA) of the acceptor bacteria (474 bp, *Lower*). L, ladder (1-kb GeneRuler).

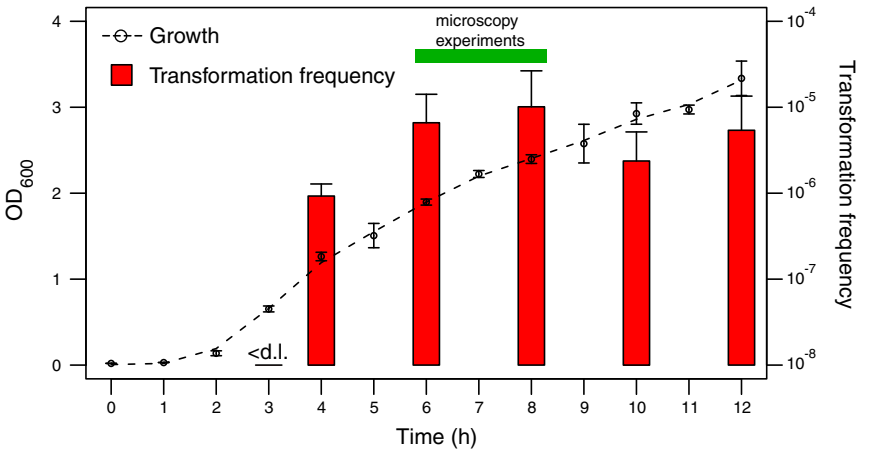

Fig. S2. Chitin-independent transformation of *V. cholerae* tested throughout different growth phases. *V. cholerae* strain A1552-Tn*tfoX* was grown in LB containing 0.02% L-arabinose (white circle). OD_{600} values and natural transformability were determined at hourly (OD_{600}) or bihourly (transformation) intervals. Smoothing splines were fitted to the experimental OD_{600} values (dashed line). Average OD_{600} values and transformation frequencies of three independent experiments ±SD are shown in the graph. The timeframe for microscopy experiments is indicated by the green bar. < d.l., below detection limit ($3.5 \times 10^{-7} \pm 3.0 \times 10^{-7}$).

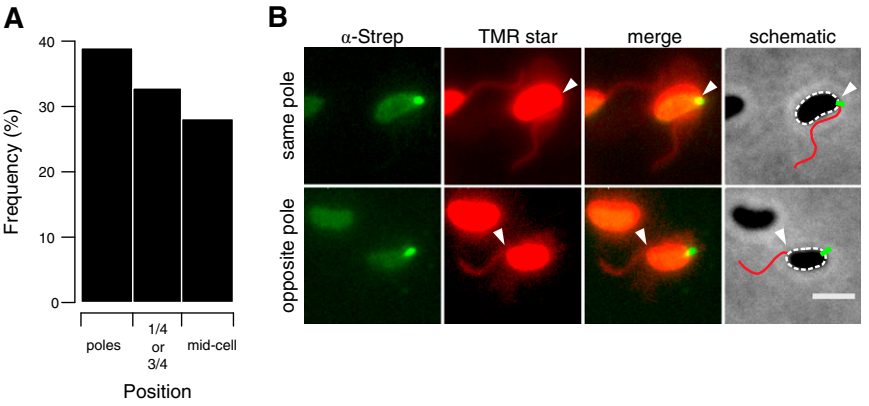

Fig. S3. Competence-induced pili are not restricted to the cell poles. Competence pili were visualized by immunofluorescence microscopy, as in Fig. 2. (*A*) A total of 5,863 bacteria were analyzed for pilus positioning in random fields of view. The relative distance of the pilus origin along the length of the cell was evaluated and is given relative to the poles, the 1/4 and 3/4 position, and the center of the cell. (*B*) Polar pilus localization is not biased toward the old or the new pole. Pili and flagella were stained in fixed cells with Oyster488-labeled anti-Strep antibodies and the SNAP-cell TMR star substrate, respectively. The origins of the flagella are highlighted with white arrowheads. Both fluorescence channels were imaged (PilA-Strep in green, TMR star in red) and superimposed (merge). A schematic representation indicating the position of the flagellum and the pilus was projected on the phase-contrast images (schematic). (Scale bar, 2 μm.)

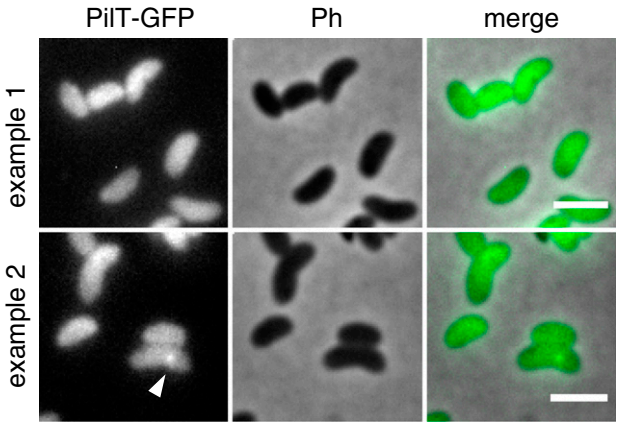

Fig. S4. The PilT protein shows a uniform cytosolic distribution pattern. The *pilT* gene, potentially encoding the cytoplasmic ATPase PilT, was replaced by the translational fusion construct *pilT-gfp*. Two representative fields of view showing several competent bacteria are shown in the fluorescent channel (PilT-GFP), in the phase-contrast channel (Ph), and as overlay between both channels (merge). Rarely observed minor foci of PilT-GFP are indicated by the white arrowhead. (Scale bars, 2 μm.)

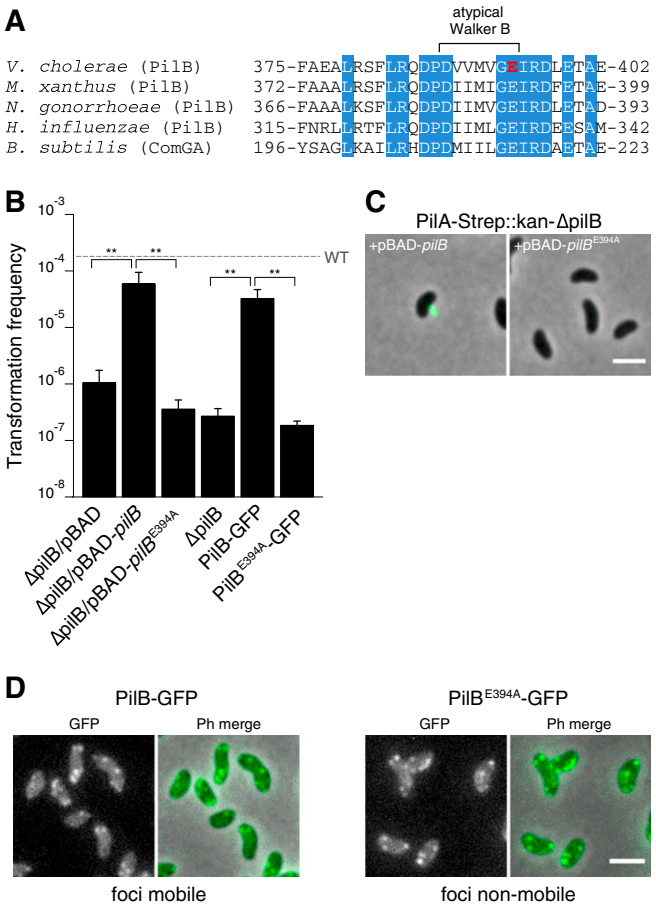

Fig. S5. The atypical Walker B motif of PilB is essential for pilus formation and natural transformation. (*A*) Alignment of the atypical Walker B motif of PilB/ComGA of different bacteria. Identical residues are highlighted in blue. The conserved residue Glu-394 within PilB of *V. cholerae* is indicated in red and was exchanged for alanine by site-directed mutagenesis (PilB^{E394A}). (*B*) Assessment of natural transformation indicates that PilB^{E394A} is nonfunctional. *pilB*^{E394A} was either expressed *in trans* from plasmid pBAD-*pilB*(E394A) or translationally fused to *gfp* [*pilB*(E394A)-*gfp*] and used to replace *pilB* on the chromosome. Both strains were tested for chitin-independent natural transformability and compared with wild-type *pilB* and *pilB*$^{-}$ strains. The transformation level of the wild-type (WT) strain is indicated by the dashed line. Shown are the averages of at least three independent experiments ±SD. Statistical significance was calculated using Welch's *t* test on log-transformed values. $^{**}P < 0.01$. (*C*) PilB^{E394A} cannot contribute to pilus biogenesis. The piliation-negative phenotype of the ΔpilB strain (carrying the *pilA-Strep* allele in place of *pilA*) (Fig. 2) could be complemented *in trans* with *pilB* (pBAD-*pilB*) but not with the site-directly mutated *pilB* variant *pilB*(E394A). Pili were visualized by immunofluorescence as described in Fig. 2. Shown are representative images. (*D*) PilB-GFP and PilB^{E394A}-GFP show a similar localization pattern within competent *V. cholerae* cells. Representative fluorescent images (GFP) and overlays with phase-contrast images (Ph merge) for both fusion proteins [PilB-GFP and PilB(E394A)-GFP; chromosomally and intraoperonally encoded] are shown. Whereas PilB-GFP foci were dynamic (Fig. 3), PilB^{E394A}-GFP foci remained static. (Scale bars, 2 μm.)

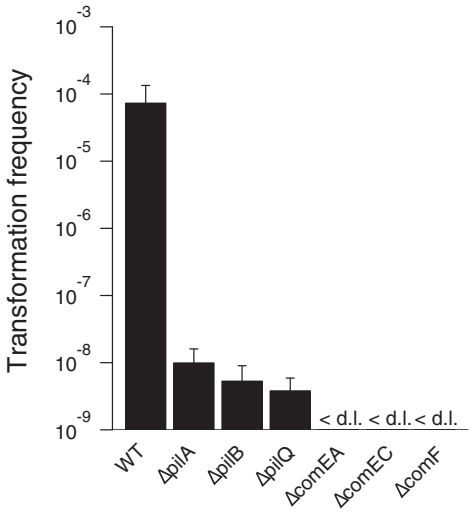

Fig. S6. Rare transformation events are detectable after chitin-mediated competence induction in Tfp mutant strains after enrichment. Chitin-induced natural transformation was performed as described in refs. 8 and 9, with minor modifications. Briefly, after detachment of the bacteria from the chitin surfaces, the cells were enriched in 2-YT (2 × Yeast extract and Tryptone) broth for 8 h before being plated and enumerated for resistant and total cfu. Shown are average transformation frequencies (±SD) of at least three independent experiments. < d.l., below detection limit, which was on average 2.9×10^{-9} ($\pm 1.2 \times 10^{-9}$).

Table S1. Genes required for efficient natural transformation of *V. cholerae*

			Homolog(s)[‡]					
Locus tag*	Gene name	Annotation[†]	N.g.	H.i	B.s.	V.p.	V.v.	V.f.
VC0462	*pilT*	Twitching motility protein PilT	*pilT*	— (*pilB*)	— (*comGA*)	*pilT*	*pilT*	*pilT*
VC0543	*recA*	recA protein	*recA*	*recA*	*recA*	*recA*	*recA*	*recA*
VC0857	*VC0857*	Pilin, putative	— (*pilV*)	— (*pilA*)	— (*comGC*)	*pilE*	*pilE*	*pilA1*
VC0858	*VC0858*	Type IV pilin, putative	— (*fimT*)	— (*comN*)	— (*comGC*)	*VP0657*	*fimT*	*VF0571*
VC0859	*VC0859*	Hypothetical protein	—	—	—	*VP0658*	*pilW*	*VF0570*
VC0860	*VC0860*	Hypothetical protein	—	—	—	*VP0659*	*VV1_0350*	*VF0569*
VC0861	*VC0861*	Type IV pilin, putative	— (*pilE*)	—	—	*VP0660*	*VV1_0349*	*VF0568*
VC1612	*VC1612*	Fimbrial biogenesis and twitching motility protein, putative	*pilW*	*pilF2*	— (*yrrB*)	*pilF*	*pilF*	*pilF*
VC1879	*comEC*	ComEC/rec2 family protein	*comA*	*rec2*	*comEC*	*rec2*	*rec2*	*comA*
VC1917	*comEA*	Conserved hypothetical protein	*comE*	*comE1*	*comEA*	*comE*	*VV1_0017*	*comE1*
VC2423	*pilA*	Fimbrial protein	*pilE*	*pilA*	*comGC*[§]	*pilA*	*pilA*	*pilA*
VC2424	*pilB*	Type IV pilus assembly protein PilB	*pilB*	*pilB*	*comGA*	*pilB*	*pilB*	*pilB*
VC2425	*pilC*	Type IV pilin biogenesis protein PilC	*pilG*	*pilC*	*comGB*	*pilC*	*vvpC*	*pilC*
VC2426	*pilD*	Leader peptidase PilD	*pilD*	*pilD*	*comC*	*pilD*	*vvpD*	*VF2188*
VC2630	*pilQ*	Fimbrial assembly protein	*pilQ*	*comE*	—	*pilQ*	*pilQ*	*pilQ*
VC2631	*pilP*	Fimbrial assembly protein pilp, putative	*pilP*	*comD*[§]	—	*pilP*	*pilP*	*VF2294*
VC2632	*pilO*	Fimbrial assembly protein pilo, putative	*pilO*	*comC*[§]	—	*pilO*	*pilO*	*pilO*
VC2633	*pilN*	Fimbrial assembly protein piln, putative	*pilN*	*comB*	—	*pilN*	*pilN*	*pilN*
VC2634	*pilM*	Fimbrial assembly protein pilm, putative	*pilM*	*comA*[§]	—	*pilM*	*pilM*	*pilM*
VC2719	*comF*	ComF family protein	*comF*	*comF*	*comFC*	*comF*	*VV1_0863*	*comF*

*The genetic organization of competence genes is indicated with arrows. VC numbers are according to ref. 1.
[†]Putative identification in *Vibrio cholerae* El Tor N16961, as listed at http://cmr.jcvi.org.
[‡]N.g., *Neisseria gonorrheae*; H.i., *Haemophilus influenzae*; B.s., *Bacillus subtilis*; V.p., *Vibrio parahaemolyticus*; V.v., *Vibrio vulnificus*; V.f., *Vibrio fischeri*. Homologs are based on protein-sequence similarities, the positions of genes in operons, and their predicted functions. If no homologs were found but BLAST hits were significant (smallest sum probability of $P < 0.01$), the best nonhomologous hit is given in parentheses.
[§]No significant BLAST hits. The indicated homology is based on predicted function or on the organization of the operon.

1. Heidelberg JF, et al. (2000) DNA sequence of both chromosomes of the cholera pathogen *Vibrio cholerae*. *Nature* 406(6795):477–483.

Table S2. *V. cholerae* strains used in this study

Strain	Genotype*	Source
A1552	Wild type, O1 El Tor Inaba; Rif^R	(1)
A1552-Tn*tfoX*	A1552 containing mini-Tn7-*araC*-P_{BAD}-*tfoX*; Rif^R, $Gent^R$	(2)
A1552-lacZ-Kan	A1552 strain with *aph* cassette in *lacZ* gene; Rif^R, Kan^R	(3)
ΔpilU (*pilT2*)	A1552 ΔVC0463::FRT; Rif^R	This study
ΔpilT	A1552 ΔVC0462::FRT; Rif^R	This study
ΔpilT-Tn*tfoX*	A1552 ΔVC0462::FRT-Tn*tfoX*; Rif^R, $Gent^R$	This study
ΔpilT ΔcomEC::kan-Tn*tfoX*	A1552 ΔVC0462 ΔVC1879::FRT-kan-FRT-Tn*tfoX*; Rif^R, $Gent^R$, Kan^R	This study
PilT-GFP	A1552 with *pilT-gfp*::FRT replacing *pilT;* Rif^R, $Gent^R$	This study
PilT-GFP-Tn*tfoX*	A1552-Tn*tfoX* with *pilT-gfp*::FRT replacing *pilT;* Rif^R, $Gent^R$	This study
ΔrecA	A1552 ΔVC0543; Rif^R	(4)
ΔrecA-Tn*tfoX*	A1552 ΔVC0543-Tn*tfoX*; Rif^R, $Gent^R$	This study
ΔrecA ΔcomEC::kan-Tn*tfoX*	A1552 ΔVC0543-ΔVC1879::FRT-kan-FRT-Tn*tfoX*; Rif^R, $Gent^R$, Kan^R	This study
ΔVC0857	A1552 ΔVC0857; Rif^R	This study
ΔVC0857-Tn*tfoX*	A1552 ΔVC0857-Tn*tfoX*; Rif^R, $Gent^R$	This study
ΔVC0857 ΔcomEC::kan-Tn*tfoX*	A1552 ΔVC0857 ΔVC1879::FRT-kan-FRT-Tn*tfoX*; Rif^R, $Gent^R$, Kan^R	This study
ΔVC0858	A1552 ΔVC0858; Rif^R	This study
ΔVC0858-Tn*tfoX*	A1552 ΔVC0858-Tn*tfoX*; Rif^R, $Gent^R$	This study
ΔVC0858 ΔcomEC-Tn*tfoX*	A1552 ΔVC0858 ΔVC1879::FRT-Tn*tfoX*; Rif^R, $Gent^R$	This study
ΔVC0859	A1552 ΔVC0859; Rif^R	This study
ΔVC0859-Tn*tfoX*	A1552 ΔVC0859-Tn*tfoX*; Rif^R, $Gent^R$	This study
ΔVC0859 ΔcomEC::kan-Tn*tfoX*	A1552 ΔVC0859 ΔVC1879::FRT-kan-FRT-Tn*tfoX*; Rif^R, $Gent^R$, Kan^R	This study
ΔVC0860	A1552 ΔVC0860; Rif^R	This study
ΔVC0860-Tn*tfoX*	A1552 ΔVC0860-Tn*tfoX*; Rif^R, $Gent^R$	This study
ΔVC0860 ΔcomEC-Tn*tfoX*	A1552 ΔVC0860 ΔVC1879::FRT-Tn*tfoX*; Rif^R, $Gent^R$	This study
ΔVC0861	A1552 ΔVC0861; Rif^R	This study
ΔVC0861-Tn*tfoX*	A1552 ΔVC0861-Tn*tfoX*; Rif^R, $Gent^R$	This study
ΔVC0861 ΔcomEC::kan-Tn*tfoX*	A1552 ΔVC0861 ΔVC1879::FRT-kan-FRT-Tn*tfoX*; Rif^R, $Gent^R$, Kan^R	This study
ΔVC1612	A1552 ΔVC1612; Rif^R	This study
ΔVC1612-Tn*tfoX*	A1552 ΔVC1612-Tn*tfoX*; Rif^R, $Gent^R$	This study
ΔVC1612 ΔcomEC::kan-Tn*tfoX*	A1552 ΔVC1612 ΔVC1879::FRT-kan-FRT-Tn*tfoX*; Rif^R, $Gent^R$, Kan^R	This study
ΔcomEC	A1552 ΔVC1879; Rif^R	(4)
ΔcomEC-Tn*tfoX*	A1552 ΔVC1879-Tn*tfoX*; Rif^R, $Gent^R$	This study
ΔcomEA	A1552 ΔVC1917; Rif^R	(5)
ΔcomEA-Tn*tfoX*	A1552 ΔVC1917-Tn*tfoX*; Rif^R, $Gent^R$	(6)
ΔcomEA ΔcomEC-Tn*tfoX*	A1552 ΔVC1917 ΔVC1879-Tn*tfoX*; Rif^R, $Gent^R$	This study
ΔpilA	A1552 ΔVC2423; Rif^R	(5)
ΔpilA-Tn*tfoX*	A1552 ΔVC2423-Tn*tfoX*; Rif^R, $Gent^R$	This study
ΔpilA ΔcomEC-Tn*tfoX*	A1552 ΔVC2423 ΔVC1879-Tn*tfoX*; Rif^R, $Gent^R$	This study
PilA-Strep-Tn*tfoX*	A1552-Tn*tfoX* with *pilA-strep*::FRT replacing *pilA;* Rif^R, $Gent^R$	This study
PilA-FRT-Tn*tfoX*	A1552-Tn*tfoX* with *pilA*::FRT replacing *pilA;* Rif^R, $Gent^R$	This study
PilA-Strep::kan-Tn*tfoX*	A1552-Tn*tfoX* with *pilA-strep*::FRT-kan-FRT replacing *pilA;* Rif^R, $Gent^R$, Kan^R	This study
PilA-Strep::kan ΔrecA-Tn*tfoX*	A1552-*pilA-strep*::FRT-kan-FRT ΔVC0543-Tn*tfoX;* Rif^R, $Gent^R$, Kan^R	This study
PilA-Strep::kan ΔpilT-Tn*tfoX*	A1552-*pilA-strep*::FRT-kan-FRT ΔVC0462-Tn*tfoX;* Rif^R, $Gent^R$, Kan^R	This study
PilA-Strep::kan ΔVC0857-Tn*tfoX*	A1552-*pilA-strep*::FRT-kan-FRT ΔVC0857-Tn*tfoX;* Rif^R, $Gent^R$, Kan^R	This study
PilA-Strep::kan ΔVC0858-Tn*tfoX*	A1552-*pilA-strep*::FRT-kan-FRT ΔVC0858-Tn*tfoX;* Rif^R, $Gent^R$, Kan^R	This study
PilA-Strep::kan ΔVC0859-Tn*tfoX*	A1552-pilA-strep::FRT-kan-FRT ΔVC0859-Tn*tfoX;* Rif^R, $Gent^R$, Kan^R	This study
PilA-Strep::kan ΔVC0860-Tn*tfoX*	A1552-*pilA-strep*::FRT-kan-FRT ΔVC0860-Tn*tfoX;* Rif^R, $Gent^R$, Kan^R	This study
PilA-Strep::kan ΔVC0861-Tn*tfoX*	A1552-*pilA-strep*::FRT-kan-FRT ΔVC0861-Tn*tfoX;* Rif^R, $Gent^R$, Kan^R	This study
PilA-Strep::kan ΔVC1612-Tn*tfoX*	A1552-*pilA-strep*::FRT-kan-FRT ΔVC1612-Tn*tfoX;* Rif^R, $Gent^R$, Kan^R	This study
PilA-Strep::kan ΔcomEC-Tn*tfoX*	A1552-*pilA-strep*::FRT-kan-FRT ΔVC1879-Tn*tfoX;* Rif^R, $Gent^R$, Kan^R	This study
PilA-Strep::kan ΔcomEA-Tn*tfoX*	A1552-*pilA-strep*::FRT-kan-FRT ΔVC1917-Tn*tfoX;* Rif^R, $Gent^R$, Kan^R	This study
PilA-Strep::kan ΔpilB-Tn*tfoX*	A1552-*pilA-strep*::FRT-kan-FRT ΔVC2424-Tn*tfoX;* Rif^R, $Gent^R$, Kan^R	This study
PilA-Strep::kan ΔpilC-Tn*tfoX*	A1552-*pilA-strep*::FRT-kan-FRT ΔVC2425::FRT-Tn*tfoX;* Rif^R, $Gent^R$, Kan^R	This study
PilA-Strep::kan ΔpilQ-Tn*tfoX*	A1552-*pilA-strep*::FRT-kan-FRT ΔVC2630-Tn*tfoX;* Rif^R, $Gent^R$, Kan^R	This study
PilA-Strep::kan ΔpilP-Tn*tfoX*	A1552-*pilA-strep*::FRT-kan-FRT ΔVC2631::FRT-Tn*tfoX;* Rif^R, $Gent^R$, Kan^R	This study
PilA-Strep::kan ΔpilO-Tn*tfoX*	A1552-*pilA-strep*::FRT-kan-FRT ΔVC2632::FRT-Tn*tfoX;* Rif^R, $Gent^R$, Kan^R	This study
PilA-Strep::kan ΔpilN-Tn*tfoX*	A1552-*pilA-strep*::FRT-kan-FRT ΔVC2633::FRT-Tn*tfoX;* Rif^R, $Gent^R$, Kan^R	This study
PilA-Strep::kan ΔpilM-Tn*tfoX*	A1552-*pilA-strep*::FRT-kan-FRT ΔVC2634::FRT-Tn*tfoX;* Rif^R, $Gent^R$, Kan^R	This study
PilA-Strep::kan ΔcomF-Tn*tfoX*	A1552-*pilA-strep*::FRT-kan-FRT ΔVC2719-Tn*tfoX;* Rif^R, $Gent^R$, Kan^R	This study
mCherry-pilQ_PilA-Strep::kan-Tn*tfoX*	A1552-*pilA-strep*::FRT-kan-FRT-*mCherry-pilQ*::FRT-Tn*tfoX;* Rif^R, $Gent^R$, Kan^R	This study
ΔpilB	A1552 ΔVC2424; Rif^R	(5)
ΔpilB-Tn*tfoX*	A1552 ΔVC2424-Tn*tfoX*; Rif^R, $Gent^R$	This study
ΔpilB ΔcomEC::kan-Tn*tfoX*	A1552 ΔVC2424 ΔVC1879::FRT-kan-FRT-Tn*tfoX*; Rif^R, $Gent^R$, Kan^R	This study

Table S2. Cont.

Strain	Genotype*	Source
PilB-GFP	A1552 with *pilB-gfp*::FRT replacing *pilB;* Rif^R, $Gent^R$	This study
PilB-GFP-Tn*tfoX*	A1552-Tn*tfoX* with *pilB-gfp*::FRT replacing *pilB;* Rif^R, $Gent^R$	This study
$PilB^{E394A}$-GFP-Tn*tfoX*	A1552-Tn*tfoX* with $pilB^{E394A}$-GFP::FRT replacing *pilB*; Rif^R, $Gent^R$	This study
ΔpilC	A1552 ΔVC2425::FRT; Rif^R	This study
ΔpilC-Tn*tfoX*	A1552 ΔVC2425::FRT-Tn*tfoX*; Rif^R, $Gent^R$	This study
ΔpilC ΔcomEC::kan-Tn*tfoX*	A1552 ΔVC2425::FRT ΔVC1879::FRT-kan-FRT-Tn*tfoX*; Rif^R, $Gent^R$, Kan^R	This study
ΔpilD	A1552 ΔVC2426::FRT; Rif^R	This study
ΔpilQ	A1552 ΔVC2630; Rif^R	(5)
ΔpilQ-Tn*tfoX*	A1552 ΔVC2630-Tn*tfoX*; Rif^R, $Gent^R$	This study
ΔpilQ ΔcomEC-Tn*tfoX*	A1552 ΔVC2630 ΔVC1879-Tn*tfoX*; Rif^R, $Gent^R$	This study
mCherry-pilQ-Tn*tfoX*	A1552-Tn*tfoX* with *mCherry-pilQ*::FRT replacing *pilQ;* Rif^R, $Gent^R$	This study
mCherry-pilQ-pilB-GFP-Tn*tfoX*	A1552-*mCherry-pilQ*::FRT (replacing *pilQ*) *pilB-gfp*::FRT (replacing *pilB*) Tn*tfoX;* Rif^R, $Gent^R$	This study
ΔpilP	A1552 ΔVC2631::FRT; Rif^R	This study
ΔpilP-Tn*tfoX*	A1552 ΔVC2631::FRT-Tn*tfoX*; Rif^R, $Gent^R$	This study
ΔpilP ΔcomEC-TntfoX	A1552 ΔVC2631::FRT ΔVC1879-Tn*tfoX*; Rif^R, $Gent^R$	This study
ΔpilO	A1552 ΔVC2632::FRT; Rif^R	This study
ΔpilO-Tn*tfoX*	A1552 ΔVC2632::FRT-Tn*tfoX*; Rif^R, $Gent^R$	This study
ΔpilO ΔcomEC::kan-Tn*tfoX*	A1552 ΔVC2632::FRT ΔVC1879::FRT-kan-FRT-Tn*tfoX*; Rif^R, $Gent^R$, Kan^R	This study
ΔpilN	A1552 ΔVC2633::FRT; Rif^R	This study
ΔpilN-Tn*tfoX*	A1552 VC2633::FRT-Tn*tfoX*; Rif^R, $Gent^R$	This study
ΔpilN ΔcomEC-Tn*tfoX*	A1552 ΔVC2633::FRT ΔVC1879-Tn*tfoX*; Rif^R, $Gent^R$	This study
ΔpilM	A1552 ΔVC2634::FRT; Rif^R	This study
ΔpilM-Tn*tfoX*	A1552 ΔVC2634::FRT-Tn*tfoX*; Rif^R, $Gent^R$	This study
ΔpilM ΔcomEC::kan-Tn*tfoX*	A1552 ΔVC2634::FRT ΔVC1879::FRT-kan-FRT-Tn*tfoX*; Rif^R, $Gent^R$, Kan^R	This study
ΔcomF	A1552 ΔVC2719; Rif^R	This study
ΔcomF-Tn*tfoX*	A1552 ΔVC2719-Tn*tfoX*; Rif^R, $Gent^R$	This study
ΔcomF ΔcomEC::kan-Tn*tfoX*	A1552 ΔVC2719 ΔVC1879::FRT-kan-FRT-Tn*tfoX*; Rif^R, $Gent^R$, Kan^R	This study
ΔmshA	A1552 ΔmshA::FRT; Rif^R	This study
ΔpilA ΔmshA	A1552 ΔpilA ΔmshA::FRT; Rif^R	This study
ΔpilA ΔmshA-Tn*tfoX*	A1552 ΔpilA ΔmshA::FRT-Tn*tfoX*; Rif^R, $Gent^R$	This study
ΔtcpA	A1552 ΔtcpA::FRT; Rif^R	This study
ΔpilA ΔtcpA	A1552 ΔpilA ΔtcpA::FRT; Rif^R	This study
ΔpilA ΔtcpA-Tn*tfoX*	A1552 ΔpilA ΔtcpA::FRT-Tn*tfoX*; Rif^R, $Gent^R$	This study
ΔVPI-1	A1552 ΔVPI-1::FRT; whole *Vibrio* pathogenicity island 1 was deleted; Rif^R	(7)
ΔVPI-1 ΔmshA	A1552 ΔVPI-1::FRT ΔmshA::FRT; Rif^R	This study
ΔpilA ΔmshA ΔVPI-1	A1552 ΔpilA ΔmshA::FRT ΔVPI-1::FRT; Rif^R	This study
ΔpilA ΔmshA ΔVPI-1 –Tn*tfoX*	A1552 ΔpilA ΔmshA::FRT ΔVPI-1::FRT-Tn*tfoX*; Rif^R, $Gent^R$	This study

*VC numbers are according to ref. 8.

1. Yildiz FH, Schoolnik GK (1998) Role of *rpoS* in stress survival and virulence of *Vibrio cholerae*. *J Bacteriol* 180(4):773–784.
2. Lo Scrudato M, Blokesch M (2012) The regulatory network of natural competence and transformation of *Vibrio cholerae*. *PLoS Genet* 8(6):e1002778.
3. Marvig RL, Blokesch M (2010) Natural transformation of *Vibrio cholerae* as a tool—optimizing the procedure. *BMC Microbiol* 10:155.
4. Suckow G, Seitz P, Blokesch M (2011) Quorum sensing contributes to natural transformation of *Vibrio cholerae* in a species-specific manner. *J Bacteriol* 193(18):4914–4924.
5. Meibom KL, Blokesch M, Dolganov NA, Wu C-Y, Schoolnik GK (2005) Chitin induces natural competence in *Vibrio cholerae*. *Science* 310(5755):1824–1827.
6. Lo Scrudato M, Blokesch M (2013) A transcriptional regulator linking quorum sensing and chitin induction to render *Vibrio cholerae* naturally transformable. *Nucleic Acids Res* 41(6): 3644–3658.
7. Blokesch M (2012) TransFLP – a method to genetically modify *V. cholerae* based on natural transformation and FLP-recombination. *J Vis Exp* 68:e3761.
8. Heidelberg JF, et al. (2000) DNA sequence of both chromosomes of the cholera pathogen *Vibrio cholerae*. *Nature* 406(6795):477–483.

Table S3. *V. cholerae* plasmids used in this study

Plasmids	Description	Source
pBAD/Myc-HisA	pBR322-derived arabinose inducible expression vector; *ara*BAD promoter (P_{BAD}); Amp^R	Invitrogen
pUX-BF13	*ori*R6K, helper plasmid with Tn7 transposition function; Amp^R	(1)
pGP704-Sac28	Suicide vector; *ori* R6K; *sacB*; Amp^R	(2)
pGP704-28-SacB-ΔVC0857	pGP704-Sac28 with a gene fragment resulting in a deletion within VC0857	This study
pGP704-28-SacB-ΔVC0858	pGP704-Sac28 with a gene fragment resulting in a deletion within VC0858	This study
pGP704-28-SacB-ΔVC0859	pGP704-Sac28 with a gene fragment resulting in a deletion within VC0859	This study
pGP704-28-SacB-ΔVC0860	pGP704-Sac28 with a gene fragment resulting in a deletion within VC0860	This study
pGP704-28-SacB-ΔVC0861	pGP704-Sac28 with a gene fragment resulting in a deletion within VC0861	This study
pGP704-28-SacB-ΔVC1612	pGP704-Sac28 with a gene fragment resulting in a deletion within VC1612	This study
pGP704-28-SacB-ΔVC2719	pGP704-Sac28 with a gene fragment resulting in a deletion within VC2719	This study
pGP704-mTn7-araC-tfoX	pGP704 with mini-Tn7 carrying *araC* and P_{BAD}-driven *tfoX*; Amp^R	(3)
pBAD-*pilA*	*pilA* cloned into NcoI/EcoRI sites of pBAD/Myc-HisA; Amp^R	This study
pBAD-*pilA-strep*	*pilA* cloned into NcoI/EcoRI sites of pBAD/Myc-HisA; Amp^R	This study
pBAD-*pilB*	*pilB* cloned into NcoI/EcoRI sites of pBAD/Myc-HisA; a SmaI site was introduced before the *pilB* stop codon; Amp^R	This study
pBAD-$pilB^{E394A}$	derived from pBAD-*pilB*; E394A point mutation encoding sequence introduced by inverse PCR; Amp^R	This study
pBAD-*pilB-gfp*	*gfp* preceded by a sequence encoding a 5-aa linker cloned into the SmaI site of pBAD-*pilB*; Amp^R	This study
pBAD-$pilB^{E394A}$-*gfp*	Derived from pBAD-*pilB-gfp*; E394A point mutation encoding sequence introduced by inverse PCR; Amp^R	This study
pBAD-*pilC*	*pilC* cloned into NcoI/EcoRI sites of pBAD/Myc-HisA; Amp^R	This study
pBAD-*pilT*	*pilT* cloned into blunted NcoI/EcoRI sites of pBAD/Myc-HisA; a SmaI site was introduced before the *pilT* stop codon; Amp^R	This study
pBAD-*pilT-gfp*	*gfp* preceded by a sequence encoding a 5-aa linker cloned into SmaI site of pBAD-*pilT*; Amp^R	This study
pBAD-*VC1612*	*VC1612* cloned into NcoI/XhoI sites of pBAD/Myc-HisA; Amp^R	This study
pBAD-*pilM*	*pilM* cloned into NcoI/EcoRI sites of pBAD/Myc-HisA; Amp^R	This study
pBAD-*pilN*	*pilN** cloned into NcoI/EcoRI sites of pBAD/Myc-HisA; Amp^R	This study
pBAD-*pilO*	*pilO** cloned into blunted NcoI/EcoRI sites of pBAD/Myc-HisA; Amp^R	This study
pBAD-*pilP*	*pilP* cloned into NcoI/EcoRI sites of pBAD/Myc-HisA; Amp^R	This study
pBAD-*pilQ*	*pilQ** cloned into NcoI/XhoI sites of pBAD/Myc-HisA; Amp^R	This study
pBAD-SacI-*pilQ*	Derived from pBAD-*pilQ* by inverse PCR; a SacI site was introduced after the sequence predicted to encode the PilQ sec-dependent signal peptide cleavage site; Amp^R	This study
pBAD-*mCherry-pilQ*	*mCherry* proceeded by a SacI site and followed by a sequence encoding a 3-aa linker plus a second SacI site was cloned into pBAD-SacI-*pilQ*; Amp^R	This study
pBAD-*VC0857*	*VC0857* cloned into NcoI/EcoRI sites of pBAD/Myc-HisA; Amp^R	This study
pBAD-*VC0858*	*VC0858** cloned into NcoI/EcoRI sites of pBAD/Myc-HisA; Amp^R	This study
pBAD-*VC0859*	*VC0859* cloned into NcoI/EcoRI sites of pBAD/Myc-HisA; Amp^R	This study
pBAD-*VC0860*	*VC0860** cloned into NcoI/EcoRI sites of pBAD/Myc-HisA; Amp^R	This study
pBAD-*VC0861*	*VC0861* cloned into NcoI/EcoRI sites of pBAD/Myc-HisA; Amp^R	This study
pBAD-*comEC*	*comEC** cloned into blunted NcoI/EcoRI sites of pBAD/Myc-HisA; a SmaI site was introduced before the *comEC* stop codon; a SacI site was introduced before the *comEC* start codon; Amp^R	This study
pBAD-*comEA*	*comEA* cloned into NcoI/EcoRI sites of pBAD/Myc-HisA; Amp^R	(4)
pBAD-*comF*	*comF* cloned into blunted NcoI/EcoRI sites of pBAD/Myc-HisA; Amp^R	This study
pBAD-recA	*recA* cloned into NcoI/EcoRI sites of pBAD/Myc-HisA; Amp^R	This study

*The predicted noncanonical start codon was exchanged for the canonical start codon *ATG*.

1. Bao Y, Lies DP, Fu H, Roberts GP (1991) An improved Tn*7*-based system for the single-copy insertion of cloned genes into chromosomes of gram-negative bacteria. *Gene* 109(1):167–168.
2. Meibom KL, et al. (2004) The *Vibrio cholerae* chitin utilization program. *Proc Natl Acad Sci USA* 101(8):2524–2529.
3. Lo Scrudato M, Blokesch M (2012) The regulatory network of natural competence and transformation of *Vibrio cholerae*. *PLoS Genet* 8(6):e1002778.
4. Lo Scrudato M, Blokesch M (2013) A transcriptional regulator linking quorum sensing and chitin induction to render *Vibrio cholerae* naturally transformable. *Nucleic Acids Res* 41(6): 3644–3658.

Table S4. Chitin-induced natural transformation assay of *V. cholerae* mutant strains

Mutant strain	Transformation frequency*	Detection limit
ΔpilT	<d.l.	1.9×10^{-8} ($\pm 1.1 \times 10^{-8}$)
ΔrecA	<d.l.	7.4×10^{-8} ($\pm 2.0 \times 10^{-8}$)
ΔVC0857	8.9×10^{-6} ($\pm 2.0 \times 10^{-6}$)	—
ΔVC0858	<d.l.	7.6×10^{-8} ($\pm 5.9 \times 10^{-8}$)
ΔVC0859	1.8×10^{-8} ($\pm 1.7 \times 10^{-8}$)†	—
ΔVC0860	7.0×10^{-7} ($\pm 1.7 \times 10^{-7}$)	—
ΔVC0861	<d.l.	4.8×10^{-8} ($\pm 9.1 \times 10^{-9}$)
ΔVC1612	<d.l.	1.3×10^{-7} ($\pm 5.7 \times 10^{-8}$)
ΔcomEC	<d.l.	9.0×10^{-8} ($\pm 5.1 \times 10^{-8}$)
ΔcomEA	<d.l.	1.3×10^{-7} ($\pm 6.0 \times 10^{-8}$)
ΔpilA	<d.l.	9.8×10^{-8} ($\pm 2.0 \times 10^{-8}$)
ΔpilB	<d.l.	6.7×10^{-8} ($\pm 2.2 \times 10^{-8}$)
ΔpilC	<d.l.	3.6×10^{-7} ($\pm 3.0 \times 10^{-7}$)
ΔpilD	n.d.‡	—
ΔpilQ	<d.l.	1.3×10^{-7} ($\pm 8.4 \times 10^{-8}$)
ΔpilP	<d.l.	7.6×10^{-7} ($\pm 7.0 \times 10^{-7}$)
ΔpilO	<d.l.	2.8×10^{-7} ($\pm 1.2 \times 10^{-7}$)
ΔpilN	<d.l.	4.9×10^{-7} ($\pm 3.4 \times 10^{-7}$)
ΔpilM	<d.l.	7.0×10^{-8} ($\pm 2.3 \times 10^{-8}$)
ΔcomF	<d.l.	1.0×10^{-7} ($\pm 7.5 \times 10^{-8}$)
ΔVC0463	1.2×10^{-4} ($\pm 9.4 \times 10^{-5}$)	—

*Transformation frequencies were determined as described in refs. 8 and 9. Shown are average transformation frequencies/detection limits (d.l.) ± SD of at least three independent experiments. The average transformation frequency of the wild-type strain was 3.5×10^{-4} ($\pm 2.1 \times 10^{-4}$).

†The transformation frequency was below the detection limit in one of three experiments.

‡n.d., not determined; the knockout strain has a significant growth defect.

Table S5. *V. cholerae* mutant strains can be complemented *in trans*

	Transformation frequency‡		
Strain†	Vector control	Complemented	Significance§
ΔpilA	1.4×10^{-6} ($\pm 1.2 \times 10^{-6}$)	1.2×10^{-5} ($\pm 3.3 \times 10^{-6}$)	**
ΔpilB	1.1×10^{-6} ($\pm 6.9 \times 10^{-7}$)	5.9×10^{-5} ($\pm 3.6 \times 10^{-5}$)	**
ΔpilC	9.6×10^{-7} ($\pm 7.9 \times 10^{-7}$)	6.8×10^{-6} ($\pm 4.8 \times 10^{-6}$)	*
ΔpilT	8.8×10^{-8} ($\pm 3.2 \times 10^{-8}$)	1.5×10^{-5} ($\pm 3.5 \times 10^{-6}$)	**
ΔVC1612	1.0×10^{-6} ($\pm 6.5 \times 10^{-7}$)	4.3×10^{-5} ($\pm 2.6 \times 10^{-5}$)	**
ΔpilM	1.2×10^{-6} ($\pm 6.7 \times 10^{-7}$)	1.3×10^{-4} ($\pm 5.3 \times 10^{-5}$)	**
ΔpilN	2.3×10^{-6} ($\pm 5.8 \times 10^{-7}$)	5.9×10^{-5} ($\pm 5.1 \times 10^{-5}$)	*
ΔpilO	4.6×10^{-7} ($\pm 2.1 \times 10^{-7}$)	1.5×10^{-4} ($\pm 7.9 \times 10^{-5}$)	**
ΔpilP	1.5×10^{-6} ($\pm 3.4 \times 10^{-7}$)	7.2×10^{-6} ($\pm 2.9 \times 10^{-6}$)	*
ΔpilQ	1.2×10^{-6} ($\pm 8.6 \times 10^{-7}$)	6.6×10^{-6} ($\pm 3.2 \times 10^{-6}$)	*
ΔVC0857	6.2×10^{-7} ($\pm 2.2 \times 10^{-7}$)	6.7×10^{-5} ($\pm 4.6 \times 10^{-5}$)	*
ΔVC0858	9.7×10^{-7} ($\pm 5.7 \times 10^{-7}$)	3.7×10^{-6} ($\pm 8.7 \times 10^{-7}$)	*
ΔVC0859	1.4×10^{-6} ($\pm 2.2 \times 10^{-7}$)	1.7×10^{-5} ($\pm 8.9 \times 10^{-6}$)	*
ΔVC0860	1.0×10^{-6} ($\pm 2.1 \times 10^{-7}$)	5.8×10^{-6} ($\pm 3.6 \times 10^{-6}$)	*
ΔVC0861	1.1×10^{-6} ($\pm 5.8 \times 10^{-7}$)	1.1×10^{-5} ($\pm 9.3 \times 10^{-6}$)	*
ΔcomEA	<d.l.¶	1.7×10^{-4} ($\pm 8.4 \times 10^{-5}$)	**,‖
ΔcomEC	<d.l.¶	1.2×10^{-4} ($\pm 9.8 \times 10^{-6}$)	**,‖
ΔcomF	<d.l.¶	4.3×10^{-5} ($\pm 2.0 \times 10^{-5}$)	**,‖
ΔrecA	<d.l.¶	5.9×10^{-6} ($\pm 4.2 \times 10^{-6}$)	**,‖

†All strains harbor the Tn*tfoX* transposon for the induction of competence.

‡Shown are average transformation frequencies ±SD for at least three independent biological experiments.

§Statistical significance was tested with Welch's *t* test on log-transformed values. *$P < 0.05$; **$P < 0.01$.

¶Detection limits (d.l.) were 8.4×10^{-8} ($\pm 2.1 \times 10^{-8}$), 9.4×10^{-8} ($\pm 1.5 \times 10^{-8}$), 5.9×10^{-8} ($\pm 1.2 \times 10^{-8}$), and 1.2×10^{-7} ($\pm 4.2 \times 10^{-8}$) for ΔcomEA, ΔcomEC, ΔcomF, and ΔrecA, respectively.

‖Detection limits were used for statistical analysis.

Table S6. Quantification of surface-exposed pili in mutant strains of *V. cholerae*

Strain*	$N^{\dagger}$	Piliated, %	1 pilus, %‡	2 pili, %‡	>2 pili, %‡
PilA-Strep::kan	3,212	5.3	96.4	3.6	0
PilA-Strep::kan ΔpilT	3,787	14.0	81.3	15.7	3.0
PilA-Strep::kan/pBAD-*pilB*	2,958	11.0	90.8	8.0	1.2

*All strains harbor the Tn*tfoX* transposon for the induction of competence.
†Number of cells analyzed.
‡Percentage of piliated cells with one, two, or more than two pili per cell.

Table S7. Natural transformation tests to validate the functionality of the translational fusion constructs

		Transformation frequency*	
Construct	Tn*tfoX* on chromosome	Chitin dependent	Chitin independent
WT	–	4.1×10^{-4} ($\pm 2.7 \times 10^{-4}$)	–
PilA::FRT	–	2.8×10^{-4} ($\pm 1.0 \times 10^{-4}$)	–
PilA::Strep	–	1.6×10^{-4} ($\pm 1.3 \times 10^{-4}$)	–
PilB-GFP	–	2.6×10^{-4} ($\pm 1.1 \times 10^{-4}$)	–
PilT-GFP	–	4.8×10^{-5} ($\pm 9.1 \times 10^{-6}$)	–
WT	+	–	1.9×10^{-4} ($\pm 7.3 \times 10^{-5}$)
PilA::FRT	+	–	4.9×10^{-5} ($\pm 1.7 \times 10^{-5}$)
PilA::Strep	+	–	5.3×10^{-6} ($\pm 6.4 \times 10^{-6}$)
PilB-GFP	+	–	3.2×10^{-5} ($\pm 1.4 \times 10^{-5}$)
PilT-GFP	+	–	6.2×10^{-6} ($\pm 1.0 \times 10^{-6}$)
mCherry-PilQ	+	–	1.6×10^{-4} ($\pm 5.1 \times 10^{-5}$)
sfGFP-PilQ	+	–	1.1×10^{-4} ($\pm 2.4 \times 10^{-5}$)
ComEA-mCherry	+	–	1.2×10^{-4} ($\pm 1.1 \times 10^{-5}$)
ComEA-sfGFP	+	–	1.9×10^{-5} ($\pm 6.0 \times 10^{-6}$)

*The average transformation frequency of at least three independent experiments ±SD is shown.